Electron transport in highly compensated, undeformed n-type InSb in the temperature range 4.2—300 K

Hari Kishan,* S. K. Agarwal,* and K. D. Chaudhuri
Department of Physics and Astrophysics, University of Delhi, Delhi 110007, India
(Received 4 November 1982)

Measurements of Hall coefficient, dc conductivity, and magnetoresistances have been made on highly compensated, undeformed n-type InSb samples from liquid helium to room temperature. The measurements show that the extent of the impurity-band conduction depends considerably on the compensation ratio and the effective concentration of the carriers. Two activation energies have been identified in the impurity-conduction region. The magnetoresistance at 4.2 K is due to impurity-band conduction and is found to be positive. It shows approximately a square-law dependence on a magnetic field. The observed behavior of magnetoresistance at 300 and 77.4 K is consistent with the behavior expected for free electrons. The variation of $\Delta\rho/\rho$ with temperature in the range 4.2—300 K at 0.3 kG is essentially governed by the variation of μ_H in the same temperature range.

I. INTRODUCTION

The study of dislocations in semiconductors is of interest for two reasons. On the one hand, the important electrical properties are much more sensitive to the dislocation content than in the case of metals, and thus it is important to know the extent to which the dislocations limit these properties. Conversely, a study of the electrical effects makes available more detailed information on the structure of the dislocations. InSb, which can be easily grown into single crystals, provides an easy access for such studies. This semiconductor on slight deformation produces an appreciable density, i.e., about 10^7 dislocations per cm^2. These are rows of atoms with unsaturated dangling bonds on the edges of extra half-planes created throughout the body of the crystal. In 60° dislocations in InSb, where In atoms are at the edge of the extra half-planes, there is no excess of electrons, and such rows will create an acceptor level in the forbidden gap. When Sb atoms form these rows, each atom has a saturated electron pair and the dislocations should introduce a donor level. These dislocations called, respectively, In and Sb type, have in effect been observed to exhibit both donor and acceptor behavior.[1,2] High-temperature plastic bending was used by Bell, Latkowski, and Willoughby[1] to introduce into indium antimonide single crystals an excess of dislocations having either In atoms at the edge of their extra half-planes or having Sb atoms there. Hall coefficient and electrical conductivity measurements, made on bent samples, indicated that both In and Sb dislocations act as an acceptor center in n-type material, and that In dislocations act as acceptor centers in p-type material. The observations on transport properties relating to plastically bent InSb samples have been taken mainly from room temperature to liquid-nitrogen temperature. An extension of these studies to liquid-helium temperatures is likely to be rewarding. With this objective in view, we have taken four different single crystals of n-type indium antimonide and we report here the results of measurements of electrical properties of these samples before deformation from 4.2 to 300 K. The studies regarding changes produced in electrical properties after deformation will be reported in a separate communication.

The conductivity of a semiconductor is very much dependent on doping, and the low-temperature conductivity of a doped semiconductor is significantly affected by the nature of the impurity band (IB), which in turn, depends[3–5] on the nature and concentration of the impurity, degree of compensation, and effective mass of the charge carriers. In order to understand the mechanism of charge transport and the nature of the scattering process, the relative contribution of free electrons and impurity-band conduction should be estimated as a function of temperature for various locations of the Fermi level. The fundamentals of the physical theory of impurity-band conduction and its phenomenological models have been discussed by a number of workers.[3,4,6–8] Since the critical concentration for Mott's transition[9] is lower in semiconductors having low effective mass, several phenomena correlated with impurity-band, e.g., metal-to-nonmetal transition[9] and hopping conduction at low temperature, are more important for semiconductors having low effective mass of the charge carriers, e.g., n-type GaAs and InSb.

At high temperature, the current is mainly carried by free charge carriers in thermal equilibrium with impurity atoms. The conductivity due to impurity-band conduction, being very small, does not normally compete with free charge-carrier conductivity except at sufficiently low temperatures. However, in semiconductors having a high degree of compensation and high energy gap, the contribution of impurity-band conduction may be significant even at high temperature.[10–15] This work reports conductivity, Hall mobility, and magnetoresistance measurements in degenerate and highly compensated samples of *n*-type InSb.

II. EXPERIMENTAL DETAILS

The electrical resistivity and Hall-coefficient measurements were made on a number of *n*-type InSb single crystals. Table I provides the relevant details of the specimens studied. The samples, after being properly cleaned by ultrasonic cleaning in propanol, were subjected to a slow lapping process using a fine mesh of corborundum power. A 1:1 HNO_3:HF solution was used for etching the lapped samples. The etched samples were washed with deionized water and ohmic contacts were then made by placing small In dots at the proper places of measurements and heating them in a furnace at ~ 170 °C in an inert atmosphere. The current contacts were spread over the entire area of the cross section of samples to avoid the possible asymmetry in the potential distribution in the sample. The voltage and Hall contacts were kept to as small a minimum as possible, ~ 0.5 mm in diameter.

The electron-transport measurements on the specimens were taken by mounting them on a copper sample holder, which was kept under vacuum in a conventional liquid-helium cryostat.[16] An electronic temperature controller[17] was used to regulate and control the temperature of the sample holder from 4.2–300 K. The ohmicity of the sample contacts was also checked. An Au + 0.03 at. % Fe versus chromel thermocouple was used to measure the temperature in the entire range of measurement. The calibration of the thermocouple was also checked periodically. A Honeywell potentiometer (Model 2783) coupled with a Leeds-Northrup null detector and a Philips dc microvoltmeter (Model PP 9004) were used to measure the potential difference across the voltage leads, the Hall voltage leads, and voltage developed in the thermocouple. A constant current generator[18] was used to pass a current ~ 1 mA through the samples. A Varian electromagnet, capable of giving a maximum of 14-kG field was used to generate the magnetic field at the specimen site for Hall voltage and magnetoresistance

TABLE I. Details of the specimens.

Samples	Dimensions (mm^3)	Resistivity ρ (10^{-4} Ω cm)			Hall coefficient R_H (cm^3/C) at 0.3 kG			Hall mobility μ_H (equal to $R_H\sigma$) (cm^2/V sec) at 0.3 kG		
		300 K	77.4 K	4.2 K	300 K	77.4 K	4.2 K	300 K	77.4 K	4.2 K
1	11×2×1	25	550	3238	199.98	7.1×10^4	6.9×10^4	8.0×10^4	1.3×10^6	2.1×10^5
2	13×3×1	42	625	4471	537.89	5.0×10^4	6.0×10^4	1.3×10^5	8.0×10^5	1.3×10^5
3	11×3×1	47	193	420	398.50	3.9×10^3	3.2×10^3	8.5×10^4	2.0×10^5	7.6×10^4
4	13×5×1	30	1020	6845	507.20	9.9×10^4	9.0×10^4	1.7×10^5	9.7×10^5	1.3×10^5

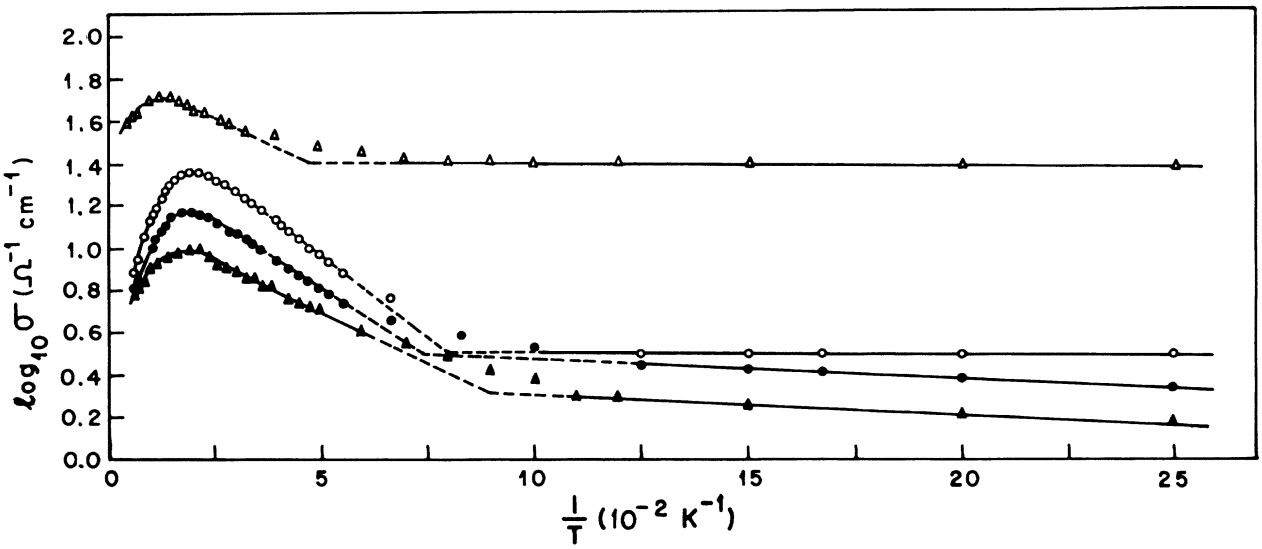

FIG. 1. Plot of $\log_{10}\sigma$ vs $1/T$ in the temperature range 4.2—100 K; sample 1, 0; sample 2, ●; sample 3, △; sample 4, ▲.

measurements. σ, R_H, and $\Delta\rho/\rho$ measurements have been carried out from 4.2—300 K in a maximum of 9-kG field, while these have been carried out up to 14 kG at three fixed points, viz. helium point, nitrogen point, and room temperature. The current through the samples and the magnetic field were also reversed while taking observations to keep to a minimum the effects of thermoelectric and thermomagnetic voltages.

III. RESULTS AND DISCUSSION

A. Conductivity

The variation of the measured conductivity with temperature ($\log_{10}\sigma$ vs $1/T$) for the samples 1, 2, 3, and 4 is shown in Fig. 1 in the temperature range 4.2—100 K. It is observed that at low temperatures this variation of the conductivity with temperature is characterized by two straight lines having two distinct slopes. The conductivity, therefore, varies according to the relation

$$\sigma=\sigma_0\exp(-\epsilon/kT)\ , \tag{1}$$

where σ_0 is the conductivity in the limit $1/T\rightarrow 0$ and ϵ is the activation energy of the thermally activated process. The two slopes indicate two different activation energies, ϵ_2 and ϵ_3. The activation energies ϵ_2 and ϵ_3 in meV are shown in Table II for all the four samples. It will be seen from Fig. 1 that there is a temperature maximum Tm up to which $\log_{10}\sigma$ vs $1/T$ is a straight line. After that, the conductivity deviates from the exponential behavior with temperature (up to about 90 K depending on the sample) showing the predominance of ionized impurity scattering. Normal free-electron lattice scattering process appears to dominate the conduc-

TABLE II. Details of the activation energies obtained from electrical conductivity data. T_{max} is the maximum temperature after which the plot of $\log_{10}\sigma$ vs $1/T$ deviates from a straight line, I temperature region starts from about 10—12 K down to helium temperatures, σ_{03} is the preexponential factor, and ϵ_3 is the activation energy in this region; II temperature region starts from T_{max} and extends down to about 18 K, σ_{02} is the preexponential factor and ϵ_2 is the activation energy in this region.

	I temperature region		II temperature region		
Samples	σ_{03} ($\Omega^{-1}cm^{-1}$)	ϵ_3 (meV)	σ_{02} ($\Omega^{-1}cm^{-1}$)	ϵ_2 (meV)	T_{max} (K)
1	3.33	0.04	43.65	2.60	29
2	3.85	0.21	25.70	2.40	32
3	25.00	0.02	65.16	1.50	59
4	2.51	0.20	15.49	1.95	33

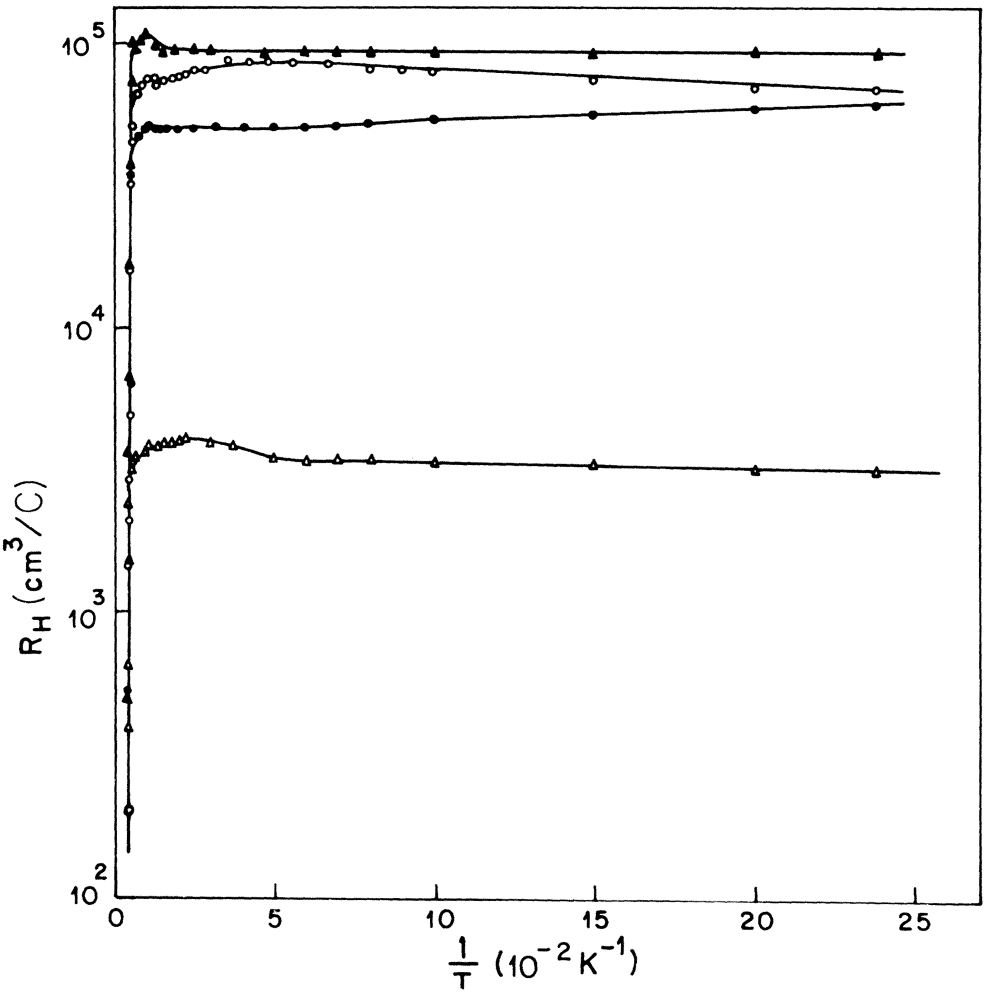

FIG. 2. Plot of Hall coefficient R_H vs $1/T$ in the temperature range 4.2–300 K at 0.3 kG; sample 1, ○; sample 2, ●; sample 3, △; sample 4, ▲.

tion phenomena above 100 K.

The variation of Hall coefficient with temperature (R_H vs $1/T$) is shown in Fig. 2. The observed Hall coefficient is characteristic of a degenerate semiconductor. At such a degenerate level the Hall scattering factor r is expected to be unity, and the concentration of the free electrons can be estimated from the measured R_H and is indicated in Table III.

It will be seen from Table III that the concentration n of free electrons varies approximately between 10^{14} and 10^{15} cm^{-3} depending on the nature of the sample. In an n-type semiconductor, if the doping is below the Mott's transition limit, the low-temperature conduction is characterized by an activation energy which is correlated to the energy differences between the ground state of the donor impurity and an impurity band which comes into existence in the forbidden energy gap near the impurity level. The low-temperature conduction in this case takes place by the thermally activated tun-

TABLE III. Details of the impurity concentration in the reported samples. n_i is the free-carrier concentration at 300 K, n is the free-carrier concentration in the flat region in the plot of R_H vs $1/T$, N_I is the concentration of ionized impurities, N_D and N_A are donor and acceptor concentrations, and $C=N_A/N_D$ is the compensation ratio.

Samples	n_i (cm^{-3})	n (cm^{-3})	N_I (cm^{-3})	N_D (cm^{-3})	N_A (cm^{-3})	$C=N_A/N_D$
1	3.68×10^{16}	8.66×10^{13}	4.16×10^{14}	2.51×10^{14}	1.65×10^{14}	0.66
2	1.37×10^{16}	1.47×10^{14}	1.06×10^{15}	6.03×10^{14}	4.56×10^{14}	0.76
3	1.85×10^{16}	2.10×10^{15}	2.04×10^{16}	1.12×10^{16}	9.15×10^{15}	0.82
4	1.45×10^{16}	7.96×10^{13}	8.01×10^{14}	4.40×10^{14}	3.61×10^{14}	0.82

neling of electrons from neutral donor atoms to ionized ones. The activation energy varies between 1.50—2.60 meV in all our samples. If the compensation is appreciable (0.66—0.82), the Fermi level is located in the impurity band, and the low-temperature conduction is due to thermally assisted hopping with a very small activation energy ϵ_3. The activation energy ϵ_3 varies between 0.02—0.21 meV and is smaller than ϵ_2. This activation energy ϵ_3 is correlated to the potential barrier between the adjacent electron droplets which are formed when the metal-to-nonmetal transition takes place.

At very low temperature, or under the condition of a weak localization of the electron states in the impurity band, the conduction may not be due to the thermally activated hopping to the nearest-neighbor site, but may be due to the variable range hopping to impurity sites having equal energy in accordance with the Mott's relation,[19]

$$\sigma = A \exp(-T_0/T)^{1/4} \quad . \tag{2}$$

The parameter T_0 is related to the density of states $N(E_F)$ near the Fermi level by the relation,[20]

$$N(E_F) = \frac{16\alpha^3}{kT_0} \quad , \tag{3}$$

α being the coefficient of exponential decay of the localized wave function. In our samples, we rule out the possibility of conduction by variable range hopping because the plots of $\log_{10}\sigma$ vs $T^{-1/4}$ do not yield straight lines. On the other hand, plots of $\log_{10}\sigma$ vs $1/T$ give straight lines with two slopes suggestive of conduction taking place via the thermally activated hopping process with two activation energies ϵ_2 and ϵ_3. The preexponential factor σ_0 is found to be much smaller than σ_m, the minimum metallic conductivity of InSb. According to Mott and Davis,[21] the minimum metallic conductivity for a degenerate semiconductor is given by

$$\sigma_m = \left[\frac{6}{z^2}\right] \frac{0.06e^2}{\hbar a} \quad , \tag{4}$$

where z is the coordination number and a is the distance between the adjacent potential wells. The value of σ_m for InSb is 348 $\Omega^{-1}\,\mathrm{cm}^{-2}$. The experimental values of the preexponential factor σ_0 for all

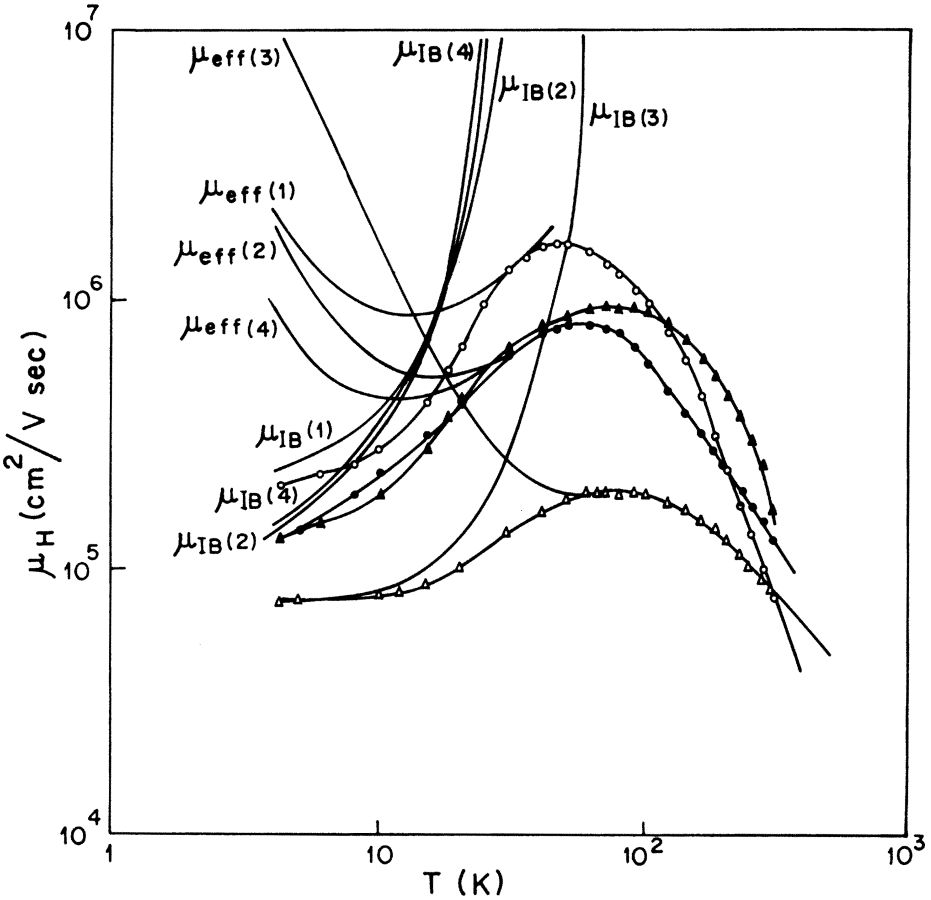

FIG. 3. Variation of observed Hall mobility μ_H vs temperature in the range 4.2—300 K at 0.3 kG; sample 1, ○; sample 2, ●; sample 3, △; sample.4, ▲; μ_{eff} and μ_{IB} are the calculated effective and impurity mobilities, and the number in parentheses refer to the sample number.

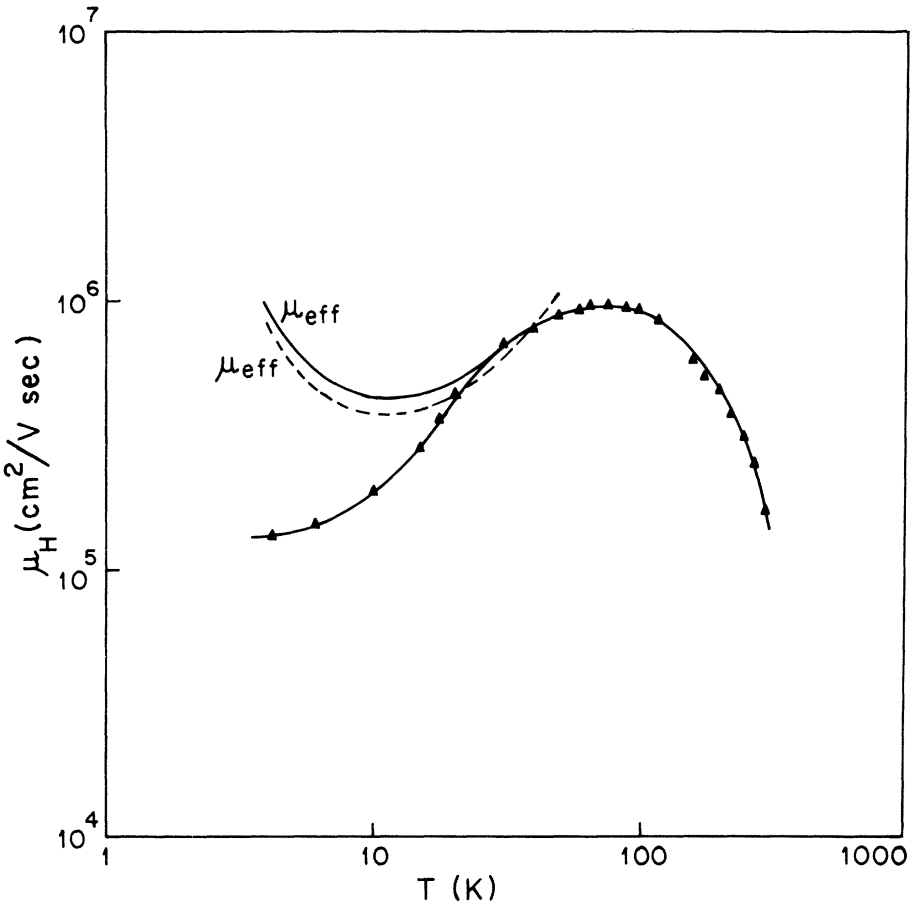

FIG. 4. Variation of Hall mobility vs temperature for sample 4; μ_{eff} (dotted curve) starts from $T_{\max}$ while μ_{eff} (solid curve) is at T_c.

the samples are much smaller than the theoretical value (Table II). It signifies that all the samples are in a nonmetallic state. The low values of the activation energies show that while the compensation in the material is enough to transform the material to a nonmetallic state, the Fermi level has not shifted outside the localized state region near the conduction-band edge.

B. Mobility

The variation of the Hall mobility with temperature in the temperature range 300—4.2 K is shown in Fig. 3. It is well known that at about the maximum of the mobility value in InSb, the relevant scattering mechanisms in InSb are deformation-potential scattering (DPS), polar optical-phonon

TABLE IV. Details of the activation energies obtained from impurity mobility data. T_c is the temperature where impurity-band conduction starts and extends down to helium temperatures, I and II temperature regions are those regions where straight lines in the plots of $\log_{10}\mu_{\text{IB}}$ vs $1/T$ are observed (Fig. 5), and $\Delta\omega_1$ is the activation energy in the I region while $\Delta\omega_2$ is the activation energy in the II region.

Samples	$\Delta\omega_1$ (meV)	$\Delta\omega_2$ (meV)	T_c (K)	ϵ_3 (meV)	ϵ_2 (meV)
1	0.27	12.8	26	0.04	2.60
2	0.44	15.6	30	0.21	2.40
3	0.05	23.1	54	0.02	1.50
4	0.39	17.6	26	0.20	1.95

scattering (OPS), and ionized impurity scattering (IIS). The values of the mobilities for the said scattering mechanisms have been calculated using the relaxation-time techniques,[22–24] and the relevant scattering parameters have been taken from Aspens[25] and Ref. 26. The value of the μ_{IIS} has been calculated by using Matthiessen's rule,

$$\frac{1}{\mu_{\text{eff}}}=\frac{1}{\mu_{\text{DPS}}}+\frac{1}{\mu_{\text{OPS}}}+\frac{1}{\mu_{\text{IIS}}}\ , \tag{5}$$

where μ_{eff} is the observed mobility at the maximum temperature up to which $\log_{10}\sigma$ vs $1/T$ is a straight line. This temperature $T_{\max}$ is chosen with the implied idea that this corresponds to the limit at which impurity band is expected to exist. This would mean that up to this temperature μ_{eff} will be equal to the observed mobility. Below this temperature relation (5) is not expected to be valid because there would be an extra mobility term due to impurity-band conduction. From this value of μ_{IIS}, the value of N_I can be calculated using the Brooks-Herring formula.[21] The concentration of donors N_D and acceptors N_A can also be calculated using $N_I=N_D+N_A$ and $n=N_D-N_A$. The values of μ_{IIS} at different temperatures can be calculated using the values of N_D and N_A from the Brooks-Herring formula. The effective mobility calculated using Eq. (5) is shown in Fig. 4 by the dotted curve labeled μ_{eff}. It is observed from this figure that the μ_{eff} intersects the observed mobility at two temperatures and the limit of the impurity band cannot be uniquely defined. The same procedure of calculat-

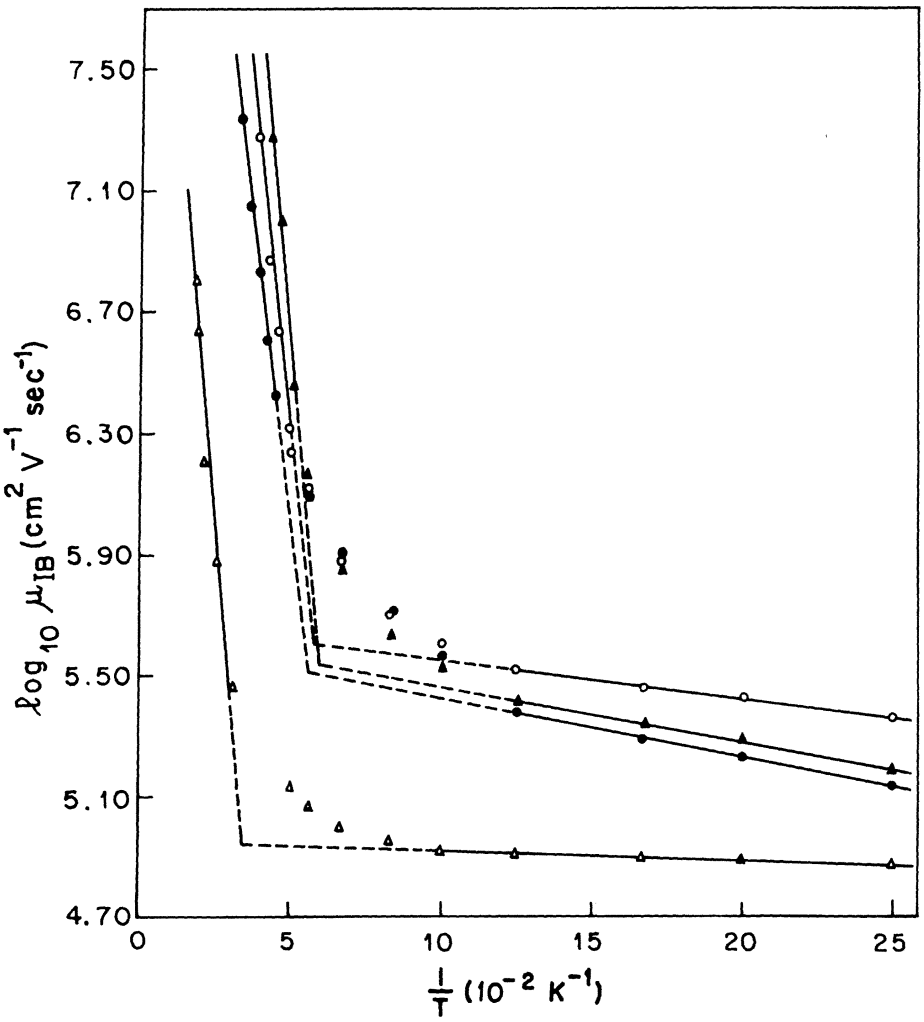

FIG. 5. Plot of $\log_{10}\mu_{IB}$ vs $1/T$ in the temperature range 4.2–100 K; sample 1, ○; sample 2, ●; sample 3, △; sample 4, ▲.

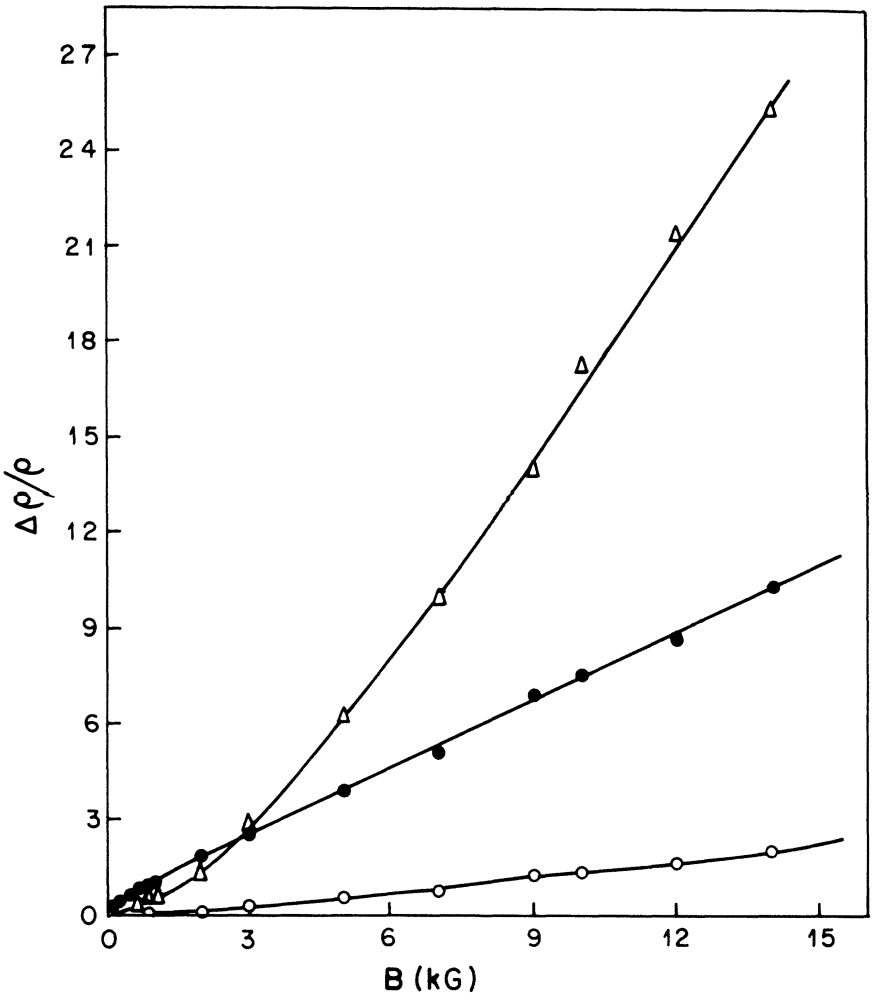

FIG. 6. Plot of $\Delta\rho/\rho$ vs magnetic field for sample 1; ○ refers at 300 K; ● at 77.4 K; △ at 4.2 K.

ing the μ_{eff} is repeated by taking temperature on the observed mobility curve below $T_{\max}$. At this temperature it is assumed that $\mu_{\text{eff}}=\mu_{\text{observed}}$. Hence μ_{IIS} can be calculated and the effective mobility can be computed at different temperatures. A situation would arise when the effective mobility computed in this manner would intersect the observed mobility curve at one particular temperature (Fig. 4, solid curve labeled μ_{eff}). This particular temperature will define the limit of temperature at which impurity-band conduction can exist. Below this critical temperature T_c, the calculated mobility values start increasing as compared to the observed mobility as the temperature is lowered (Fig. 3). This shows the existence of impurity-band conduction below the critical temperature which increases as the temperature is lowered.

The values of μ_{IB} mobility due to impurity-band conduction at various temperatures have been estimated from the relation

$$\frac{1}{\mu_{\text{IB}}}=\frac{1}{\mu_{\text{ops}}}-\frac{1}{\mu_{\text{eff}}}\ , \tag{6}$$

and these values are shown in Fig. 3. It is observed that there is a significant contribution of impurity-band conduction in the low-temperature region. It will be seen from Fig. 3 that the impurity band extends, in general, to higher temperatures if the compensation is higher, but it also depends on the effective carrier concentration. Figure 5 shows the plot of $\log_{10}\mu_{\text{IB}}$ vs $1/T$. The plot shows a linear variation with two distinct slopes. This clearly shows that μ_{IB} satisfies the relation

$$\mu_{\text{IB}}=\mu_0\exp(-\Delta\omega/kT)\ , \tag{7}$$

where $\Delta\omega$ is the activation energy for the mobility in the impurity band and μ_0 is the mobility in the limit $1/T\rightarrow 0$. The mobility activation energy for the different samples is shown in Table IV and the conductivity activation energy is also incorporated in the

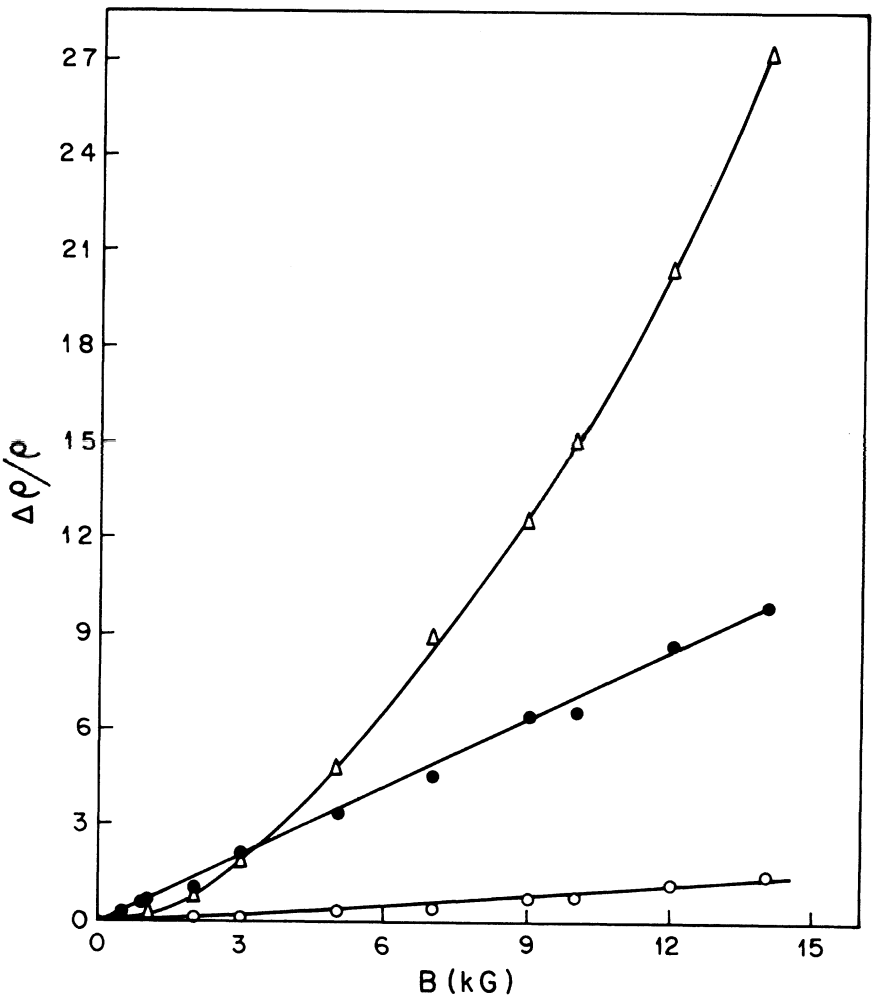

FIG. 7. Plot of $\Delta\rho/\rho$ vs magnetic field for sample 2; ○ refers at 300 K; ● at 77.4 K; △ at 4.2 K.

same table for comparison. It will be noted that the mobility activation energy is higher than the conductivity activation energy. A probable cause for this difference is that the drifting carriers are repeatedly trapped and thermally released from shallow traps during their transit. Moreover, the conductivity activation energy is obtained purely from conductivity data when there is no magnetic field, whereas the mobility activation energy is calculated from the observed Hall mobility, which, essentially implies measurement in the presence of a magnetic field. It will be noted from Tables II and IV that the temperature maximum from the $\log_{10}\sigma$ vs $1/T$ plot is higher than that from the $\log_{10}\mu_{IB}$ vs $1/T$ plot. The highest temperature at which the impurity-band conduction exists can be uniquely determined from the mobility in the impurity band; the conductivity data give a rough estimate. Therefore the temperature from the mobility data mentioned in Table IV indicates the true value of the limit of the impurity band.

C. Magnetoresistance

The magnetoresistance (MR) measurements as a function of the magnetic field, made on the samples at 300, 77.4, and 4.2 K, have been shown in Figs. 6–9. The observed MR at 300 and 77.4 K is consistent with the behavior expected for free electrons. By assuming that the variation of MR, $\Delta\rho/\rho$ is proportional to B^n, the value of n at 300 and 77.4 K is about 2 for low magnetic fields. Thus the observed

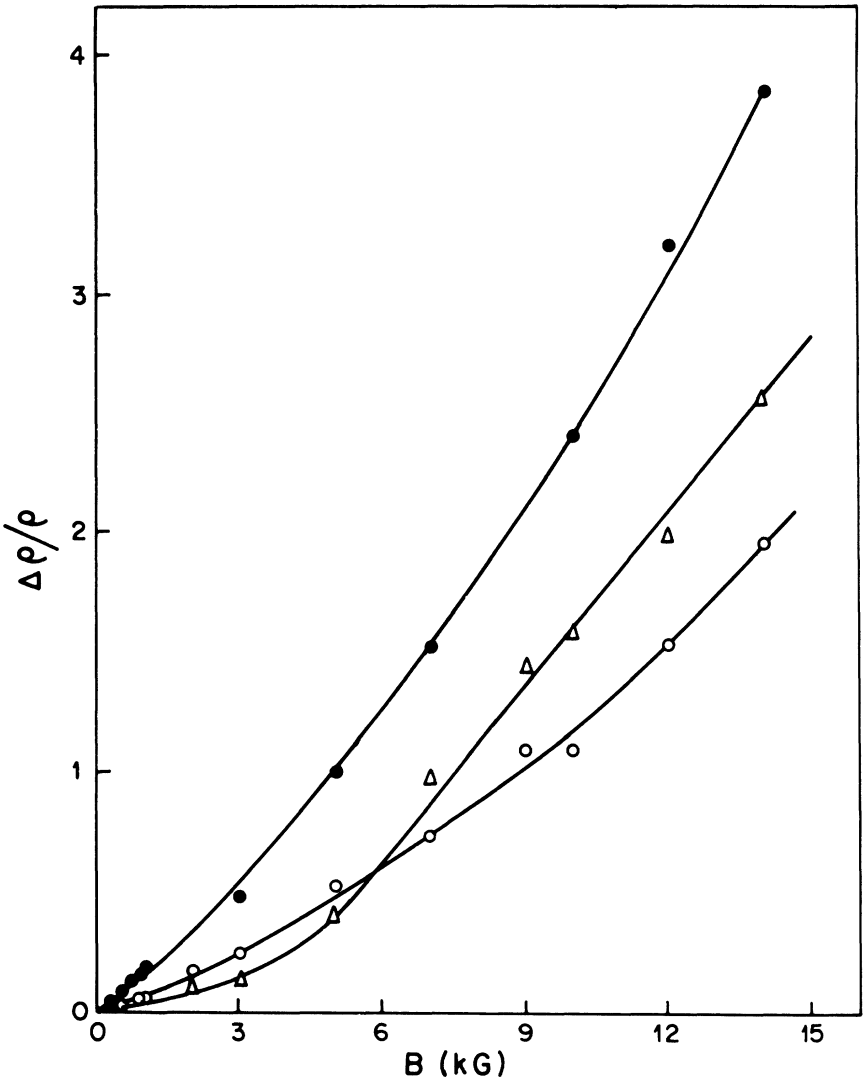

FIG. 8. Plot of $\Delta\rho/\rho$ vs magnetic field for sample 3; ○ refers at 300 K; ● at 77.4 K; △ at 4.2 K.

MR at 300 and 77.4 K gives a square-law behavior expected for free electrons, and the MR at 300 K is lower than that at 77.4 K in all the samples. For higher fields, n decreases and is about 1. This is so because MR tends to saturate at high fields. However, the MR measurements at 4.2 K show a different type of variation. For samples 1 and 2, MR at 4.2 K is higher than that at 77.4 K (Figs. 6 and 7) for values of magnetic field higher than 3 kG, but for lower values of magnetic field MR at 4.2 K is lower than that at 77.4 K. The impurity-band conduction in these two samples extend up to about 30 K. Therefore the MR at 4.2 K is governed by impurity-band conduction. On the other hand, the MR at 77.4 K is due to free carrier conduction. For samples 3 and 4, MR at 77.4 K is higher than that at 4.2 K for all values of the magnetic field (Figs. 8 and 9). It is to be noted here that the impurity-band conduction in sample 3 extends to about 50 K, and that in sample 4 to about 30 K; the MR at 4.2 K is due to impurity-band conduction but the MR at 77.4 K is due to free carrier conduction. The variation of $\Delta\rho/\rho$ with temperature in the temperature range 300—4.2 K and at 0.3 kG is shown in Fig. 10. The MR, which depends on μ, should essentially be governed by the variation of μ in the temperature range 300—4.2 K. This is generally true in all the specimens considered (Figs. 3 and 10). Various theories exist to explain the MR due to impurity-band conduction. Toyozawa[27] and Sasaki[28] ex-

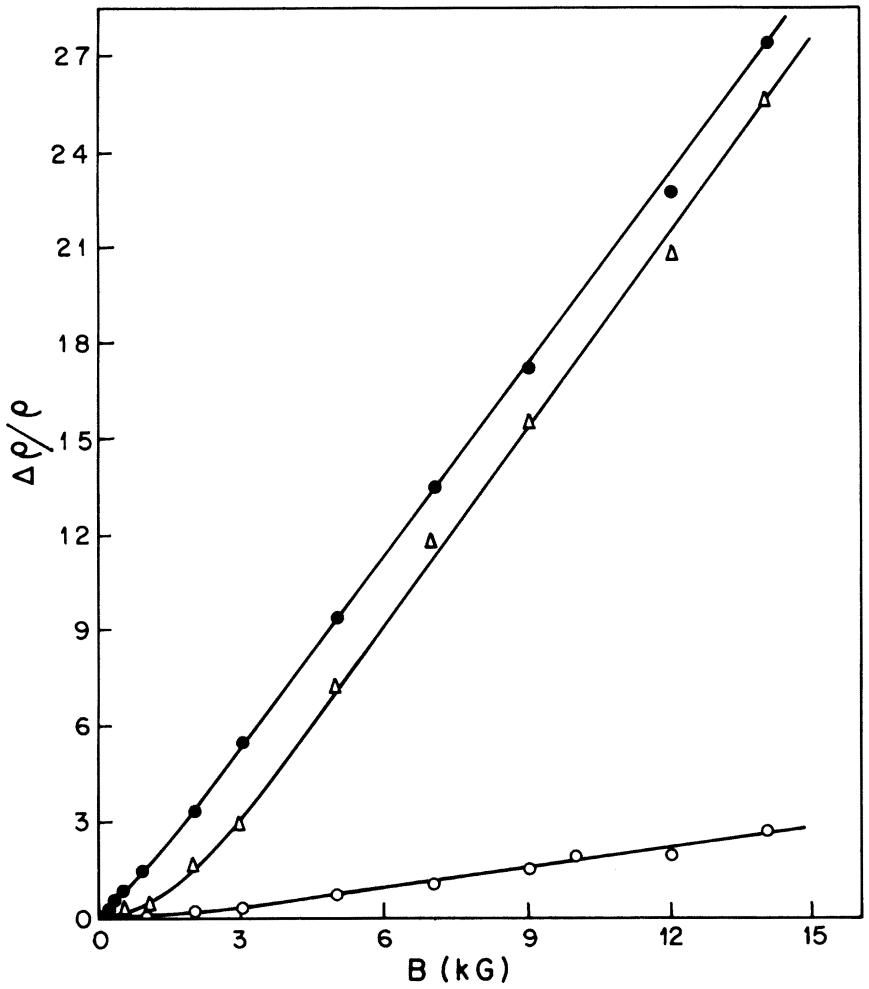

FIG. 9. Plot of $\Delta\rho/\rho$ vs magnetic field for sample 4; ○ refers at 300 K; ● at 77.4 K; △ at 4.2 K.

plained the negative MR on the basis of spin-dependent scattering. However, these theories predict a square-law dependence of negative MR on the applied magnetic field. Mott and Zinamon[9] proposed a shift of the Fermi level E_F by an amount $\pm\mu_B H$ (where μ_B is the Bohr magneton) at $T=0$ upon application of the magnetic field and expressed the magnetic field dependence of the conductivity σ by the relation,

$$\sigma=\sigma(E_F)+(\mu_B H)^2\frac{\partial^2\sigma}{\partial E^2} \quad , \tag{8}$$

so that

$$\delta\sigma=(\mu_B H)^2\frac{\partial^2\sigma}{\partial E^2} \quad , \tag{9}$$

in which the sign of $\partial^2\sigma/\partial E^2$ determines whether MR is positive or negative. This theory suggests a square-law dependence of MR on a magnetic field. The variation of MR with a magnetic field at 4.2 K follows from Eq. (9). In all our samples this is approximately true at 4.2 K. The MR is positive in all the samples. This essentially depends on the nature of the sample and on the degree of compensation. Negative MR has been observed in crystalline semiconductors at cryogenic temperatures[29,30] when the impurity concentration is above the "Mott transition limit" so as to make the impurity-band conduction possible. In the heavily doped semiconductors, when the impurity concentration is in the region of metallic impurity conduction, negative MR has also been observed even at high temperature.[31,32]

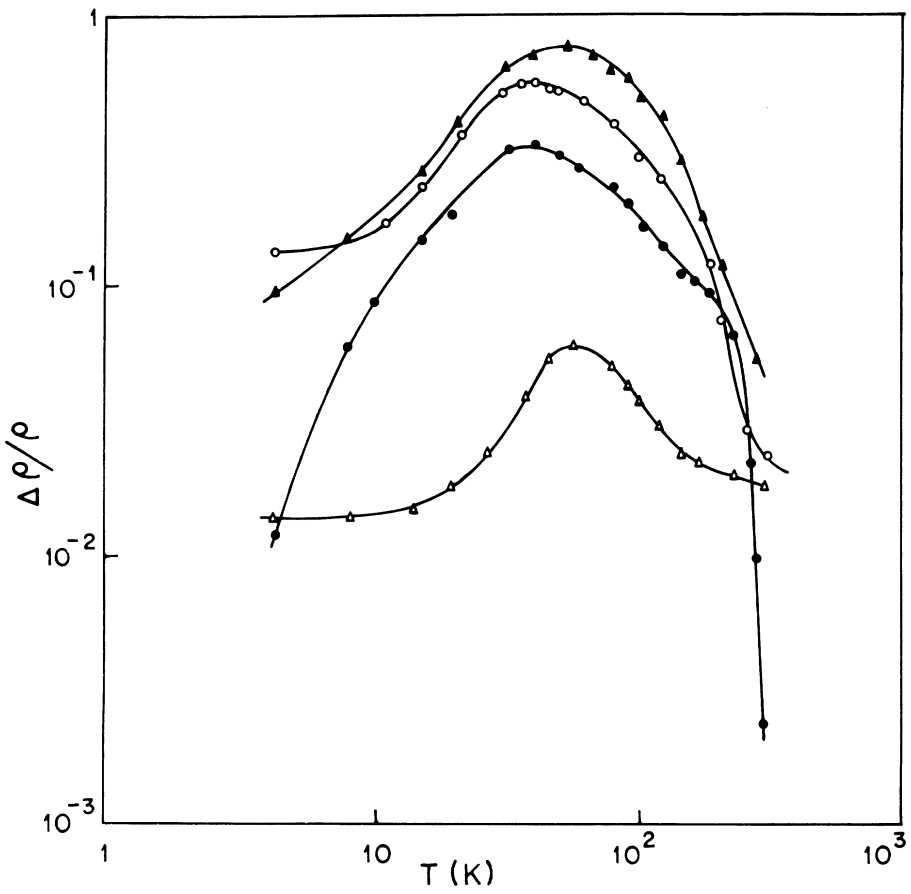

FIG. 10. Variation of magnetoresistance $\Delta\rho/\rho$ with temperature in the temperature range 4.2—300 K at 0.3 kG; sample 1, ○; sample 2, ●; sample 3, △; sample 4, ▲.

The MR in all our samples at 300 K is less than that at 77.4 K. This is consistent with the expected behavior of free electrons. The MR at 4.2 K for the four samples is apparently governed by Eq. (9) and can be very high when the magnetic field is high. This explains why the MR at 4.2 K is higher than that at 77.4 K for values of a magnetic field higher than 3 kG for samples 1 and 2.

*Present address: National Physical Laboratory, New Delhi 110012, India.

[1]R. L. Bell, R. Latkowski, and A. F. W. Willoughby, J. Mater. Sci. 1, 66 (1960).
[2]J. J. Duga, J. Appl. Phys. 33, 169 (1962).
[3]P. W. Anderson, Phys. Rev. 109, 1492 (1958).
[4]N. F. Mott and W. D. Twose, Adv. Phys. 10, 107 (1961).
[5]P. R. Rimbey and G. D. Mahan, Phys. Rev. B 10, 3419 (1974).
[6]A. Miller and F. Abrahams, Phys. Rev. 120, 745 (1960).
[7]M. Pollak and T. H. Geballe, Phys. Rev. 122, 1472 (1961).
[8]N. F. Mott, Philos. Mag. 35, 111 (1977).
[9]N. F. Mott and Z. Zinamon, Rep. Prog. Phys. 33, 881 (1970).
[10]B. R. Sethi, P. C. Mathur, and J. Woods, J. Appl. Phys. 49, 3618 (1978).
[11]B. R. Sethi, P. C. Mathur, and J. Woods, J. Appl. Phys. 50, 352 (1979).
[12]J. Frenkel, Phys. Rev. 54, 647 (1938).
[13]K. D. Chaudhuri, P. C. Mathur, T. K. Saxena, V. B. Bothra, and A. J. Malhotra, Phys. Rev. B 21, 767 (1980).
[14]T. K. Saxena, Shashi Bala, S. K. Agarwal, P. C. Mathur, and K. D. Chaudhuri, Phys. Rev. B 22, 2962 (1980).
[15]K. D. Chaudhuri, A. Luthra, P. Saxena, S. K. Agarwal, and P. C. Mathur, Phys. Rev. B 22, 6319 (1980).
[16]T. K. Dey, Ph.D. thesis, University of Delhi, 1977 (unpublished).

[17]A. K. Mukerjee, T. K. Dey, and K. D. Chaudhuri, Cryogenics 13, 243 (1973).
[18]A. K. Mukerjee and K. D. Chaudhuri, Stud. J. IETE (India) 15, 180 (1974).
[19]N. F. Mott, Philos. Mag. 19 835 (1969).
[20]V. Ambegaokar, B. I. Halperin, and J. S. Langer, Phys. Rev. B 4, 2612 (1971).
[21]N. F. Mott and E. A. Davis, *Electronic Progress in Non-crystalline Materials* (Oxford University Press, New York, 1971), p. 26.
[22]K. Seeger, *Semiconductor Physics* (Springer, New York, 1973), p. 175.
[23]D. J. Howarth and E. H. Sondheimer, Proc. R. Soc. London, Sect. A 219, 53 (1953).
[24]H. Brooks, Adv. Electron. Electron. Phys. 7, 85 (1955).
[25]D. E. Aspens, Phys. Rev. B 14, 5331 (1976).
[26]*Semiconductors and Semimetals,* edited by A. C. Beer and R. K. Willardson (Academic, New York, 1975), Vol. 10.
[27]Y. Toyozawa, J. Phys. Soc. Jpn. 17, 986 (1962).
[28]W. Sasaki, J. Phys. Soc. Jpn. 20, 825 (1965).
[29]J. F. Woods and C. Y. Chen, Phys. Rev. 135A, A1462 (1964).
[30]L. Halbo and R. J. Sladek, Phys. Rev. 173, 794 (1968).
[31]W. Sasaki and De Bruyn Ouboter, Physica (Utrecht) 27, 877 (1961).
[32]R. P. Khosla and J. R. Fisher, Phys. Rev. B 2, 4084 (1970).